Two-level model and magnetic field effects on the hysteresis in *n*-GaAs

Shwu-Yun Tsay Tzeng[1,*] and Yiharn Tzeng[2]
[1]*Department of Electro-Optical Engineering, National Taipei University of Technology, Taipei, Taiwan 106, Republic of China*
[2]*Institute of Physics, Academia Sinica, Taipei, Taiwan 115, Republic of China*
(Received 19 December 2003; revised manuscript received 29 March 2004; published 25 August 2004)

Efforts are made in this work to interpret the experimentally observed magnetic effects on the hysteretic *I*-*V* curve for an *n*-GaAs semiconductor through a two-impurity-level model with the assumptions of spatial homogeneity in current flow direction and instantaneous energy balance. We construct the model by considering carefully the Landau level shifts for the electrons in the conduction band, the magnetoresistance property, and the modification on the cross sections of the impact ionization. With the inclusions of the effects from the carrier electron temperature variation and the field-dependent electron mobility, we are able to describe the hysteretic *I*-*V* characteristics satisfactorily for the case of applying either a longitudinal or a transverse magnetic field simultaneously within a single model. Our numerical results show that when the applied longitudinal magnetic field *B* increases, the holding voltage of the hysteresis shifts towards a higher value, while the breakdown voltage remains almost fixed and thus the width of the hysteresis decreases. Above a critical magnetic field intensity 86 mT, the hysteresis vanishes. Under the transverse magnetic field, the breakdown voltage of the hysteresis shifts significantly towards the higher direction with a stronger magnetic field *B*, and therefore a considerably wider hysteresis width. The dynamic behavior of our model has displayed the same features of the experimental observations described by Aoki, Kondo, and Watanabe in Solid State Commun. **77**, 91 (1991).

DOI: 10.1103/PhysRevB.70.085208 PACS number(s): 72.20.Ht

I. INTRODUCTION

Many interesting nonlinear characteristics such as the hysteresis of the static current-voltage,[1,2] breathing filaments,[3–10] and self-sustained chaotic current or voltage oscillation[2,11–17] have been discovered in the semiconductors with an S-shaped negative differential conductivity under a dc bias voltage. A number of experimental works on the instability and chaos in *n*-GaAs induced by magnetic fields with different orientations, either transverse or longitudinal[1,18] to the electric field applied on the device, have been reported. Many of the above nonlinear transport properties can be described by the well-established two-impurity-level model.[2]

Aoki, Kondo, and Watanabe[1] investigated the effects from the external magnetic field *B* on hysteresis of an *I*-*V* curve for an *n*-GaAs semiconductor. The main features of the experimental observations are (1) when $B=0$, the system exhibits a hysteretic *I*-*V* curve; (2) if the system is under a longitudinal magnetic field, the holding voltage of the hysteresis moves towards a higher voltage for a higher *B*, while the breakdown voltage almost remains fixed. For $B>47$ mT, the holding voltage exceeds the breakdown voltage, and hysteresis fades away; and (3) when the applied *B* field is transverse, the hysteresis shifts towards a higher breakdown voltage and its width becomes wider apparently for a higher *B*.

In this paper we would like to propose a two-level model, with the assumptions of spatial homogeneity in current flow for the planar-type ohmic contacts[5] and instantaneous energy balance, along with a careful treatment on the magnetoresistance property to explain the observed characteristics of the hysteresis under the magnetic fields. Our efforts will be made not only for the case of applying a transverse magnetic field *B* but also the case of applying a longitudinal *B* to the static electric field *E* imposed in the device. We have noticed that few theoretical studies have tried to interpret the above two cases within a single model simultaneously.

In the two-level model, the electronic states of a donor impurity consist of the ground level with density n_{t_1} and the first excited level with density n_{t_2}. The carrier density *n* in the conduction band is determined by the generation-recombination (GR) processes in which an electron in these states of impurity may be thermally ionized or impact ionized to the conduction band, and may then recombine with a donor having an empty state. Processes considered in the GR are shown in Fig. 1.

The applied external magnetic field can influence the GR processes, especially the thermal ionization and the impact ionization, through several aspects. The Landau level shifts for the electrons in the conduction band, the magnetoresis-

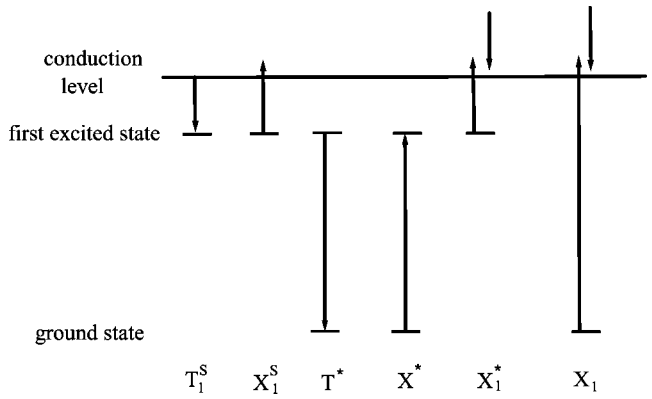

FIG. 1. Generation-recombination processes considered in the two-level model, involving the conduction band, the trap ground state, and the first excited state.

tance, and the modification on the cross sections of the impact ionization are among those needed to be considered. We will discuss them in detail in the next section. Because the conduction electron effective mass of *n*-GaAs is rather small ($\approx 0.066 m_0$), the Zeeman shifts of the bound impurity electrons are much smaller than the Landau level shifts and are thus ignored.

During the GR processes the temperature T_e of the electrons may vary a little. The increase of T_e with rising electric field has been inspected and its importance has been detailedly discussed in Refs. 19–22. The thermal ionization coefficient may thus be altered as a result of the temperature variation. We will find T_e from an energy balance equation[23] and investigate the dependence of thermal ionization upon the electric field E and the carrier density n through T_e.

Results from the numerical simulation based on the above theoretical framework preserve very nicely the main features of the previously mentioned experimental observations.[1] Properties in the case with either an external longitudinal or an external transverse magnetic field, such as the shifts of the hysteresis, the widths between the holding voltage and breakdown voltage, and the disappearance of the hysteresis in the case under a longitudinal B, can all be interpreted in our model.

This paper is organized as follows. The detailed description of our model will be given in Sec. II. Our numerical results will be presented in Sec. III. The discussion and summary follows.

II. THE MODEL

The two-level model stated in the previous section is applied to an *n*-GaAs at liquid-helium temperature. In terms of the ground level density n_{t_1}, the first excited level density n_{t_2}, and the carrier density n in the conduction band, the GR rate equations are given by[2,12]

$$\dot{\nu} = X_1 N_D^* \nu \nu_{t_1} + (X_1^s + X_1^* N_D^* \nu)\nu_{t_2} - T_1^s N_D^* (N_A/N_D^* + \nu)\nu, \tag{1}$$

$$\dot{\nu}_{t_1} = -(X^* + X_1 N_D^* \nu)\nu_{t_1} + T^* \nu_{t_2}, \tag{2}$$

with $\nu = n/N_D^*, \cdots$, etc., $N_D^* = N_D - N_A$ being the effective doping concentration, N_D, N_A the donor and the acceptor concentrations, respectively, $\nu_{t_2} = 1 - \nu - \nu_{t_1}$ from the conservation of charge, and the dot denoting the time derivative. The definitions of the GR coefficients $X_1^s, T_1^s, X_1, X_1^*, X^*$, and T^* are shown in Fig. 1, and their magnitudes at 4.2 K given in Table I.

Equations (1) and (2) have been solved at a fixed temperature,[2,12] namely, at $T = 4.2$ K. In this work, in addition to investigating effects on the system from externally applied magnetic fields, we will also consider the effect from temperature variations through the thermal ionization coefficients. In doing so, we first make the assumption that the energy relaxation occurs faster than all other processes, so that the energy relaxation time is much shorter than the dielectric field-relaxation time. Since for well-separated time-scale processes, the dynamics is dominated[2] by the slow variable and the fast variable is slaved, in our case the energy balance assumes a quasi-steady state almost instantaneously, determining the mean energy $\mathcal{E}$ of the carriers as a function of the electric field E which varies slowly.

TABLE I. The parameters corresponding to *n*-GaAs at 4.2 K for the two-level GR mechanism.

Parameter	Value
T_1^s	10^{-6} cm^3 s^{-1}
T^*	10^6 s^{-1}
X_1^s	5×10^5 s^{-1}
X^*	4.7×10^5 s^{-1}
X_1^0	5×10^{-8} cm^3 s^{-1}
X_1^{*0}	10^{-6} cm^3 s^{-1}
N_A/N_D^*	0.3
ε	$10\varepsilon_0$
m^*	$0.066 m_0$
μ_0	2.5×10^4 cm^2/V s
T_M	2.15
ν_c	1.87×10^{-2}
α	4.82×10^2
T_L	4.2 K
β_0^2	3×10^2
ν_0	5.75×10^{-3}
N_D^*	10^{15} cm^{-3}

During the GR processes the electron temperature T_e will increase and can be determined through $\mathcal{E} = \frac{3}{2} k_B T_e$ with k_B being the Boltzmann constant. $\mathcal{E}$ can be obtained from the energy balance equation[23]

$$\dot{\mathcal{E}} = -(\mathcal{E} - \mathcal{E}_L)/\tau(\mathcal{E}) + e\mu_B E^2, \tag{3}$$

where $\mathcal{E}_L = \frac{3}{2} k_B T_L$ is the thermal energy at zero-electric field with T_L the lattice temperature, $\tau(\mathcal{E}) \propto \mathcal{E}^{-1/2}$ the energy relaxation time considered theoretically, and μ_B the carrier mobility in the magnetic field.

Let us now look into possible effects on the thermal ionization coefficient due to the temperature variation. At helium temperature $T_L = 4.2$ K, $k_B T_L = 0.362$ meV is roughly in the same order as $\varepsilon_b^* = 1.5$ meV, the impurity first excited state binding energy for *n*-GaAs with shallow impurities. The thermal ionization coefficient X_1^S of the excited level contains the essential nonlinear dependencies upon the carrier density n and the electric field E. Therefore we express the dependence of thermal $X_1^S(T_e)$ upon E and n through the electron temperature T_e by multiplying a Boltzmann factor

$$X_1^S(T_e) = X_1^S(T_L) e^{\varepsilon_b^* (1/k_B T_L - 1/k_B T_e)}. \tag{4}$$

Because of the Boltzmann factor, the thermal ionization coefficient can be visibly increased as the electrons are heated to T_e.

At low temperatures, the thermal ionization probability of the impurity electrons will also be affected by the presence of the magnetic field B. We then have to take into account

the binding energy shifts of the impurity, known as the Landau level shifts for the electrons in the conduction band. Eq. (4) is thus modified as[24]

$$X_1^s(T_e,B) = X_1^s(T_e,0)e^{-\Delta\varepsilon_B/k_BT_e}, \tag{5}$$

where $X_1^s(T_e,0)=X_1^s(T_e)$ of Eq. (4), and $\Delta\varepsilon_B=\hbar\omega_c^*/2(\omega_c^*=eB/m^*c)$ is the conduction ground state Landau level shift. For n-GaAs, $m^*=0.066m_0$, $\Delta\varepsilon_B=0.877B$ meV with B in units of T (tesla). Therefore at helium temperature $T_e=4.2$ K, the modification of the Boltzmann factor in Eq. (5) appears to be significant as B is a few tenths of 1 T.

We now turn to the impact-ionization coefficients X_1 and X_1^*. In the absence of a magnetic field, X_1 and X_1^* can be approximately expressed in terms of the electric field E and the impurity ground and the first excited state binding energies ε_b and ε_b^* from the Lucky model as[25]

$$X_1(E) = X_1^0 e^{-\varepsilon_b/E}, \tag{6}$$

$$X_1^*(E) = X_1^{*0} e^{-\varepsilon_b^*/E}, \tag{7}$$

with coefficients X_1^0 and X_1^{*0} given in Table I.

When a magnetic field B is applied to the system, there will be three effects on X_1 and X_1^*. The first one is the shifts on the binding energies ε_b and ε_b^* due to the Landau level shifts of the conduction electrons. We thus replace ε_b and ε_b^* in Eqs. (6) and (7) by the magnetic field-dependent binding energies ε_b^B and ε_b^{*B} as

$$\varepsilon_b^B = \varepsilon_b + \Delta\varepsilon_B, \tag{8}$$

$$\varepsilon_b^{*B} = \varepsilon_b^* + \Delta\varepsilon_B. \tag{9}$$

$\Delta\varepsilon_B$, already defined in Eq. (5), makes ε_b^B and ε_b^{*B} shift significantly from $\varepsilon_b=6.0$ meV and $\varepsilon_b^*=1.5$ meV for n-GaAs as B is around a few tenths of 1 T.

The second one that we have to consider is the magnetoresistance under magnetic field B. Owing to the magnetoresistance the carrier mobility μ_B decreases as the magnetic field increases:

$$\mu_B = h\mu_{BH}. \tag{10}$$

For the compensated n-type GaAs, electrons are scattered by the ionized acceptors as well as by the ionized donors. To have a more accurate theory, we consider the electric field-dependent mobility of the electrons with density n at temperature T_e given by Brooks-Herring(BH)[26] as

$$\mu_{BH} = \mu_0\left(\frac{T_e}{T_L}\right)^{3/2}\frac{2N_A/N_D^* + \nu_0}{2N_A/N_D^* + \nu}\frac{\ln(1+\beta_0^2) - \beta_0^2/(1+\beta_0^2)}{\ln(1+\beta^2) - \beta^2/(1+\beta^2)}, \tag{11}$$

$$\beta^2 = \beta_0^2\left(\frac{T_e}{T_L}\right)^2\frac{\nu}{\nu_0}, \tag{12}$$

where μ_0 is the zero-electric field mobility at temperature T_L, $\nu_0=n_0/N_D^*$, and n_0 and β_0 are the electron density and the so-called BH coefficient, respectively, under the same conditions, and $\nu=n/N_D^*$, n, β for those at temperature T_e. Since T_e can be determined from the energy balance equation [Eq. (3)] and ν is related to the electric field by GR rate [Eqs. (1) and (2)], our μ_{BH} is dependent of the electron temperature and the electric field.

When a longitudinal magnetic field is applied, the current filament nucleated between two parallel ohmic contacts has been found from experiments.[22,27–30] For the observed spatial pattern,[28–30] the current flows are curved along the filament boundaries, where they may experience a Lorentz force since the current flows along the boundaries are not completely parallel to the applied longitudinal magnetic field B especially near the contacts. As a result, the inhomogeneous magnetoresistance induced at the filament boundaries should be taken into account. The thresholdlike magnetoresistance factor h is introduced for this effect and approximated as[23,31]

$$h = 1 - \frac{1}{2}T_M(\mu_0 B)^2\{1 + \tanh[\alpha(\nu - \nu_c)]\} \tag{13}$$

with T_M being the magnetoresistance scattering factor, ν_c being related to the critical density necessary for the current filamentation, and α the inhomogeneity factor of the current filament. The factor h is so chosen because from experimental observations, different properties are shown in different regimes in the current-voltage characteristic of the sample n-GaAs. In the low-conducting regime the current-density distribution is spatially uniform but in the high-conducting regime a stable current filament is formed.[32] Accordingly, in Eq. (13) the factor $h\sim 1$ for the ohmic current ($\nu \ll \nu_c$) and $h\sim 1-T_M(\mu_0 B)^2$ for the filamentary current ($\nu \gg \nu_c$).

Things go much simpler when applying a transverse magnetic field. In this case h[17,33,34] is

$$h = \frac{1}{1 + \mu_H^2 B^2}, \tag{14}$$

with μ_H being the conduction electron Hall mobility.

The third effect from B is the modification on the cross sections of X_1^0 and X_1^{*0}. As suggested in Refs. 13, 23, and 35, the cross sections of the impact ionization are proportional to $\varepsilon_i^{1/2}(1+\gamma_0\mu\sqrt{\varepsilon_i})$, with ε_i the electron binding energy and γ_0 a constant. Therefore the cross sections of X_1^0 and X_1^{*0} should be multiplied by a factor, respectively, as follows:

$$\alpha(B) = \left(\frac{\varepsilon_b^B}{\varepsilon_b}\right)^{1/2}\frac{1 + \eta h\sqrt{\varepsilon_b^B}}{1 + \eta\sqrt{\varepsilon_b}}, \tag{15}$$

$$\alpha^*(B) = \left(\frac{\varepsilon_b^{*B}}{\varepsilon_b^*}\right)^{1/2}\frac{1 + \eta h\sqrt{\varepsilon_b^{*B}}}{1 + \eta\sqrt{\varepsilon_b^*}}, \tag{16}$$

with constant $\eta=0.4$. These two factors are exactly equal to 1 as $B=0$.

Combining these three effects, the impact-ionization coefficients X_1 and X_1^* can be written as

$$X_1(E,B) = \alpha(B)X_1^0 e^{-\varepsilon_b^B h^{-1/2}/E}, \tag{17}$$

$$X_1^*(E,B) = \alpha^*(B)X_1^{*0} e^{-\varepsilon_b^{*B} h^{-1/2}/E}. \tag{18}$$

Finally since the electric field E in the circuit is related to the applied external fields, let us look into the circuit dynamics. We consider the case that a static electric field is applied in the x direction, $\boldsymbol{E}_0 = E_0\hat{\boldsymbol{x}}$, and a static magnetic field is applied either in the longitudinal x direction $\boldsymbol{B} = B\hat{\boldsymbol{x}}$ or in the transverse y direction $\boldsymbol{B} = B\hat{\boldsymbol{y}}$. The dynamical equations for the case of applying a longitudinal magnetic field can be written as

$$\dot{E}_x = -\gamma_d\left(-E_0 + E_x + \frac{AR}{L}J\right) \tag{19}$$

with the current density

$$J = e\nu N_D^* \mu_B E_x, \tag{20}$$

where $1/\gamma_d$ is the effective dielectric relaxation time, R the load resistance, and L and A are, respectively, the length and the cross-sectional area of the sample.

On the other hand, the situation is more complicated for the transverse magnetic-field case, since additionally the induced Hall field E_z has to be taken into account. In this case we have the dynamical equations with E_x taking the same form as that in Eq. (19) but with the current density as

$$J = e\nu N_D^* \mu_B (E_x + \mu_H B E_z), \tag{21}$$

and in addition,

$$\epsilon \dot{E}_z = e\nu N_D^* \mu_B (\mu_H B E_x - E_z), \tag{22}$$

$$\epsilon \dot{E}_y = -e\nu N_D^* \mu E_y. \tag{23}$$

Here $\nu N_D^* = n$ is the conduction electron density, ϵ the permittivity of the sample, and μ_B the electron mobility in the magnetic field. Note that in this case, the total current density in Eq. (21) differs from the one in Eq. (20) for the longitudinal case by an E_z dependent term.

Of course, $E^2 = E_x^2 + E_y^2 + E_z^2$ for both the longitudinal and the transverse B field cases, except that for the former only E_x exists, while for the latter E_x and E_z all exist with the steady state E_z being solved from Eq. (22) and the E_y component decaying exponentially to zero very rapidly.

III. SIMULATIONS AND NUMERICAL RESULTS

In our calculation, the energy balance equation (3) is converted to[36]

$$\dot{\overline{T}}_e = -\frac{1}{\tau_0}[\overline{T}_e^{1/2}(\overline{T}_e - 1)] + \frac{2e}{3k_B T_L}\mu_B E^2, \tag{24}$$

where $\overline{T}_e = T_e/T_L$, and the energy relaxation time constant $\tau_0 = 6.79 \times 10^{-11}$ s is considered theoretically to be much shorter than the effective dielectric relaxation time $1/\gamma_d$, typically in the order of $\approx 10^{-6}$ s.[36] During GR processes, an instantaneously quasi-steady state is assumed and the balanced temperature is derived from Eq. (24).

The numerical procedure in our simulation is as follows. We solve the fixed point of the dynamic equations (1) and (2) when all the time derivatives in the left-hand side of these two equations are zero. For a given ν, starting from a guessed $T_{e,0}$, one can find the electron mobility μ_{BH} from Eq. (11), and then has the magnetoresistance factor h either from Eq. (13) for the case with an external longitudinal B or from Eq. (14) for that with a transverse B by making the simple approximation $\mu_H = \mu_0$. We solve the electric field from Eqs. (1) and (2) through the GR coefficients, and obtain a new electron temperature $T_{e,1}$ from the energy balance equation [Eq. (24)]; repeating the iterative procedure until $T_{e,i}$ approaches a convergent value T_e. Therefore, under a certain external magnetic field B, for a given electron density ν, we have the solutions of the electron temperature T_e, the electron mobilities μ_{BH} and μ_B, and the electric field E. In this way, we can establish the ν vs E_x S-shaped electron density-electric field characteristic. Furthermore, the current density J can be obtained from either Eq. (20) for the longitudinal magnetic field, or Eq. (21) for the transverse one, respectively. Therefore the J vs E_x S-shaped current density-electric field characteristic is obtained.

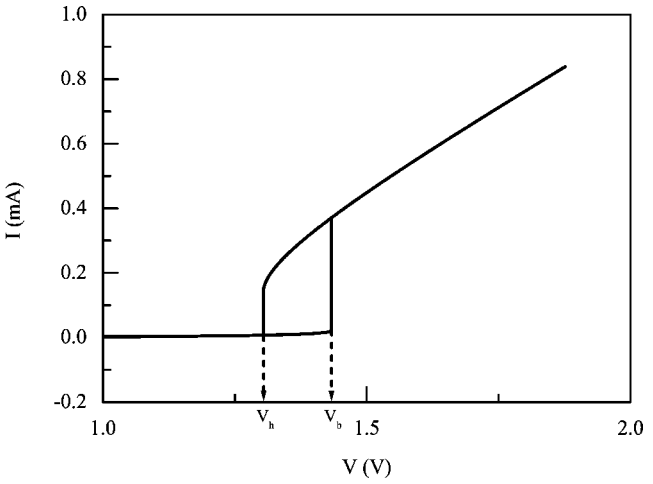

FIG. 2. The I-V curve of an S-shaped NDC n-GaAs reveals hysteretic characteristics when it is connected in series with a dc bias and a resistance R, where V is the applied voltage. The holding voltage V_h and breakdown voltage V_b are indicated.

Using the above obtained J and E_x, we can further find the relationship between the applied voltage V and current $I = JA$ for the S-shaped GaAs from the load-line condition $E_x L + JAR = V$ from Eq. (19) with a fixed resistance $R = 500\ \Omega$, the sample length $L = 0.3$ cm, and the cross-sectional area $A = 1.0 \times 10^{-4}$ cm^2 in a realistic circuit. Plotted in Fig. 2 is our I-V curve when there is no magnetic field. The hysteresis loop can clearly be seen with the holding voltage around $V_h = 1.310$ V and the breakdown voltage around $V_b = 1.433$ V, as indicated in the figure.

Our results from the case of applying a longitudinal magnetic field are shown in Fig. 3(a), where we obtained similar features as those observed experimentally by Aoki *et al.*,[1] namely, the holding voltage of the hysteresis moves towards a higher voltage for a higher B, while the breakdown voltage almost remains fixed. For $B > 86$ mT, the holding voltage exceeds the breakdown voltage and thus the hysteretic phenomenon disappears. Apparently the width of hysteresis becomes narrower for a larger B. This behavior will also be

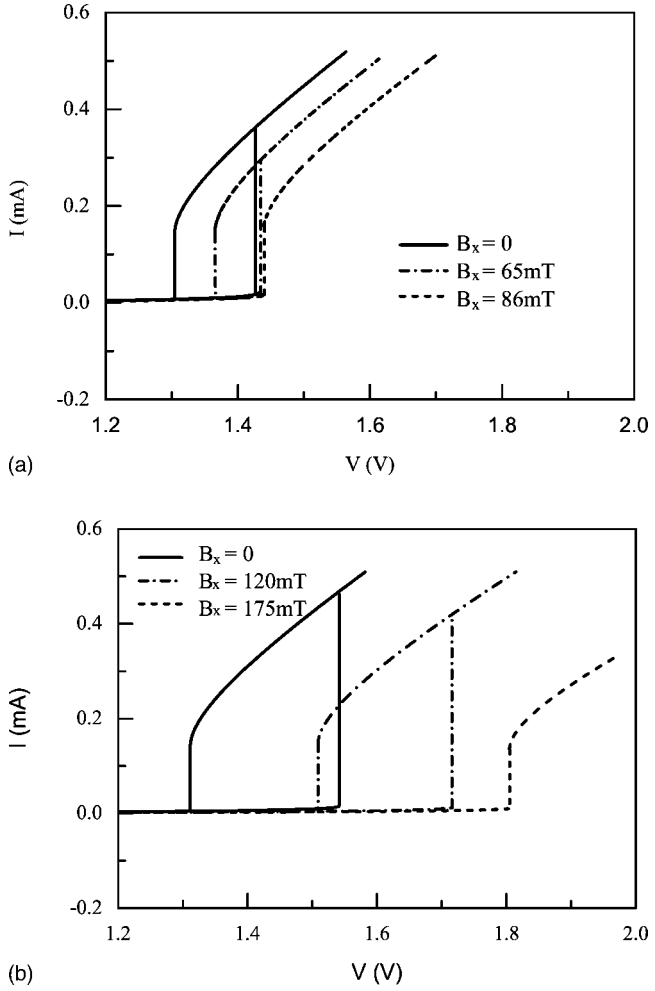

FIG. 3. *I-V* characteristics under longitudinal magnetic field B_x.(a) Including all factors considered in our model. (b) Same as in (a), except that without the modification on impact-ionization cross-section correction and the electron temperature variation, setting T_e=4.2 K.

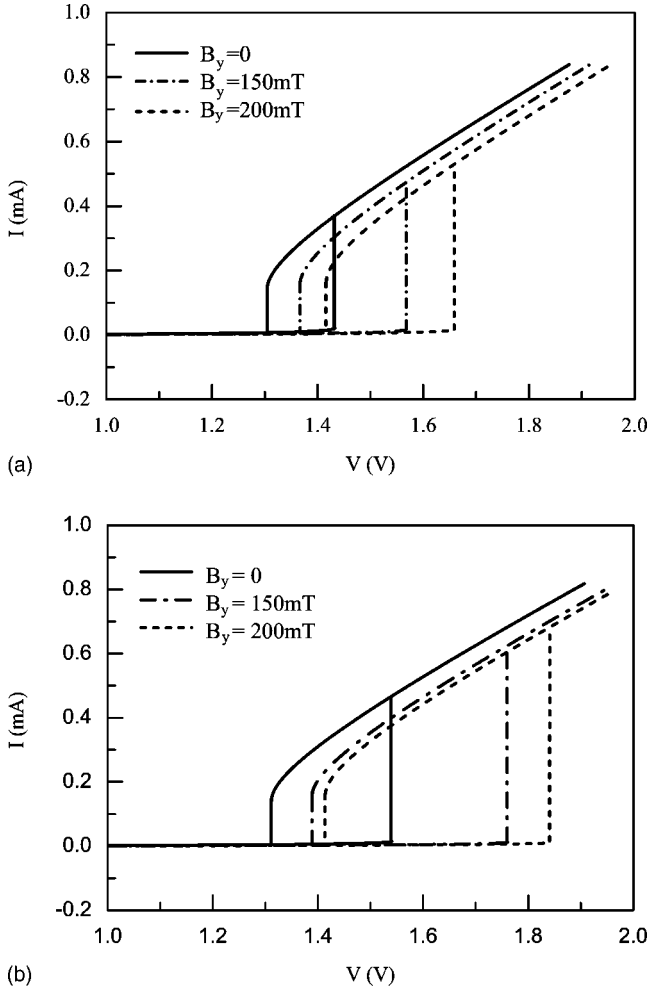

FIG. 4. Same as Fig. 3 except that the device is under transverse magnetic field B_y.

reflected in the dashed-dotted line in Fig. 5, where the ratio of the hysteresis width $\Delta V(=V_b-V_h)$ at B to that without applying magnetic field as a function of B is plotted.

We also examine separately the contributions from the variation of carrier electron temperature T_e and the modification on the cross sections of the impact ionization. Results are quite different if we exclude these two factors in the calculation, as presented in Fig. 3(b), where we see that as the longitudinal magnetic field is being raised, the breakdown voltage no longer remains unchanged but moves toward higher V and the width ΔV becomes wider than that in the curve with the same B in Fig. 3(a). The vanishing of the hysteresis occurs at B=175 mT , much larger than that in Fig. 3(a). We also find that if only excluding the contribution of T_e from conditions in Fig. 3(a), the hysteresis will disappear at B=120 mT. Hence both contributions from these two ingredients are important to keep V_b fixed and to help narrow down the width ΔV.

We now turn to the case of applying a transverse magnetic field. Shown in Fig. 4(a) are our results of the *I-V* curves for the device under a transverse B with all factors considered in our model. Unlike the longitudinal B case, here both the holding and the breakdown voltages become higher and the hysteresis width wider for higher external transverse magnetic fields. The increasing normalized width for the increas-

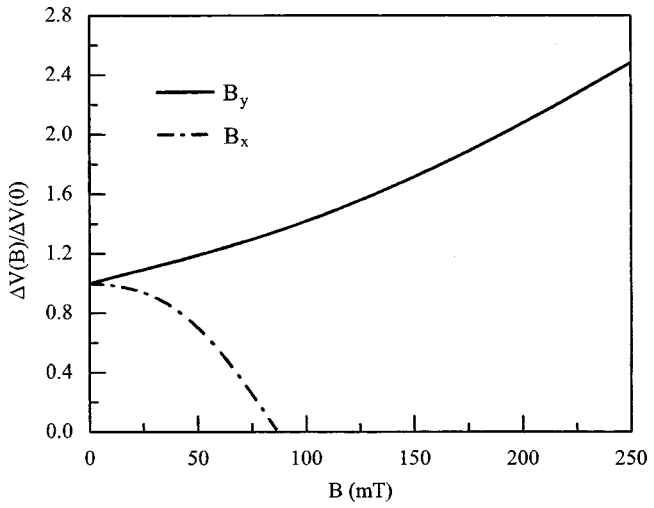

FIG. 5. Normalized hysteretic width $\Delta V(B)/\Delta V(0)$ as a function of the magnetic field intensity with $\Delta V(0)$=0.123 V.

ing B is plotted in the solid line in Fig. 5. Similarly, we also display the I-V curves obtained without considering the variation of T_e and the modification on the cross sections of the impact ionization in Fig. 4(b). Different from the situations between Figs. 3(a) and 3(b), the holding voltages do not change much between Figs. 4(a) and 4(b), but the breakdown voltages become larger and the widths get wider for curves under the same B if the above two factors are not included. The differences between the I-V curve behaviors from using longitudinal magnetic fields and from using transverse ones mainly arise from the magnetoresistance's different effects in these two cases as can be seen from Eqs. (10)–(23).

Our results in Figs. 2, 3(a), 4(a), and 5 are satisfactorily consistent with the experimental observations.[1]

IV. CONCLUSION

In summary, we have established a two-impurity-level model based on the assumptions of spatial homogeneity in the x direction and instantaneous energy balance to explain the experimentally observed hysteretic I-V curve[1] for the n-GaAs semiconductor under longitudinal and transverse magnetic fields. We carefully consider the magnetic effects through the Landau level shifts for the electrons in the conduction band, the magnetoresistance property, and the modification on the cross sections of the impact ionization. In these considerations, we adopt the electric field-dependent electron mobility μ_{BH}, rather than a constant, so that the system can be described more accurately. We also investigate the importance of carrier electron temperature T_e variation from the lattice temperature $T_L=4.2$ K.

Our numerical results describe the experimental observations[1] satisfactorily. When the device is free from any magnetic field, the system already possesses the hysteretic I-V curve. If we then switch on a longitudinal magnetic field B and increase it gradually, we find that the breakdown voltage of the hysteresis almost stays fixed while the holding voltage becomes higher and thus the width of the hysteresis turns to be narrower. As the magnetic field reaches a critical value B_c, the hysteresis vanishes. On the other hand, if the applied B field is transverse, the hysteresis moves to a higher voltage direction with both the breakdown and holding voltages becoming larger and its width wider for a higher B. All these results are in reasonably good agreement with the experimentally observed hysteretic I-V characteristics. The nice thing in this work is that we are able to interpret the experimental observations when either a longitudinal or a transverse magnetic field is applied simultaneously all within a single model.

We also study the importance of the variation of carrier electron temperature T_e and the modification on the cross sections of the impact ionization. We find that without considering these two factors, the width of hysteresis becomes wider for both cases of external magnetic fields. Moreover, the breakdown voltage in the longitudinal magnetic field case can no longer be kept fixed if any one of these two factors is excluded from consideration. Hence they together play the roles of avoiding V_b running away from an almost fixed value and also of helping narrow the width ΔV. It is clear that the contributions from these two are important in our model.

Overall, we have a simple model which describes the experimental observations satisfactorily. However, since it is a macroscopic model, we do not expect that it can also interpret all microscopic properties of the system. Moreover, our model may need some refinements from microscopic aspects.

We are working on this line and also trying to extend our theory further to examine other experimentally observed nonlinear characteristics in n-GaAs, such as instability and chaos of current under the longitudinal magnetic field for $B>B_c$. We will report the results in a future publication.

*Electronic address: sytsay@ntut.edu.tw

[1] K. Aoki, T. Kondo, and T. Watanabe, Solid State Commun. **77**, 91 (1991).
[2] E. Schöll, *Nonequilibrium Phase Transitions in Semiconductors* (Springer, Berlin, 1987).
[3] E. Schöll and D. Drasdo, Z. Phys. B: Condens. Matter **81**, 183 (1990).
[4] A. Brandl and W. Prettl, Phys. Rev. Lett. **66**, 3044 (1991).
[5] G. Hüpper, K. Pyragas, and E. Schöll, Phys. Rev. B **47**, 15 515 (1993).
[6] V. Novák, C. Wimmer, and W. Prettl, Phys. Rev. B **52**, 9023 (1995).
[7] E. Kunz and E. Schöll, Z. Phys. B: Condens. Matter **89**, 289 (1992).
[8] E. Schöll, Solid-State Electron. **32**, 1129 (1989).
[9] K. Kardell, C. Radehaus, R. Dohmen, and H.-G. Purwins, J. Appl. Phys. **64**, 6336 (1988).
[10] F. S. Lee and Y. C. Cheng, Chin. J. Phys. (Taipei) **38**, 155 (2000).
[11] R. Obermaier, W. Böhm, W. Prettl, and P. Dirnhofer, Phys. Lett. **105A**, 149 (1984).
[12] E. Schöll, Physica B & C **134**, 271 (1985).
[13] E. Schöll, J. Parisi, B. Röhricht, J. Peinke, and R. P. Huebener, Phys. Lett. A **119**, 419 (1987).
[14] M. Weispfenning, I. Hoeser, W. Böhm, W. Prettl, and E. Schöll, Phys. Rev. Lett. **55**, 754 (1985).
[15] K. Aoki, T. Kobayashi, and K. Yamamoto, J. Phys. Soc. Jpn. **51**, 2373 (1982).
[16] K. Aoki and K. Yamamoto, Phys. Lett. **98A**, 72 (1983).
[17] G. Hüpper, E. Schöll, and A. Rein, Mod. Phys. Lett. B **6**, 1001 (1992).
[18] J. Spangler, A. Brandl, and W. Prettl, Appl. Phys. A: Solids Surf. **48**, 143 (1989).
[19] M. Gaa, R. E. Kunz, and E. Schöll, Phys. Rev. B **53**, 15 971 (1995).
[20] B. Kehrer, W. Quade and E. Schöll, Phys. Rev. B **51**, 7725 (1995).

[21] H. Kostial, M. Asche, R. Hey, K. Ploog, B. Kehrer, W. Quade, and E. Schöll, Semicond. Sci. Technol. **10**, 775 (1995).
[22] M. Gaa, R. E. Kunz, E. Schöll, W. Eberle, J. Hirschinger, and W. Prettl, Semicond. Sci. Technol. **11**, 1646 (1996).
[23] K. Aoki, Phys. Lett. A **152**, 485 (1991).
[24] S. Y. T. Tzeng and Y. C. Cheng, Phys. Rev. B **68**, 035211 (2003).
[25] W. Shockley, Solid-State Electron. **2**, 35 (1961).
[26] K. Seeger, *Semiconductor Physics, An Introduction* (Springer, Berlin, 1999).
[27] V. Novák, J. Hirschinger, F.-J. Niedernostheide, W. Prettl, M. Cukr, and J. Oswald, Phys. Rev. B **58**, 13 099 (1998).
[28] K. Aoki, U. Rau, J. Peinke, J. Parisi, and R. P. Huebener, J. Phys. Soc. Jpn. **59**, 420 (1990).
[29] U. Rau, K. Aoki, J. Peinke, J. Parisi, W. Clauss, and R. P. Huebener, Z. Phys. B: Condens. Matter **81**, 53 (1990).
[30] G. Schwarz, C. Lehmann, A. Reimann, E. Schöll, J. Hirschinger, W. Prettl, and V. Novák, Semicond. Sci. Technol. **15**, 593 (2000).
[31] K. Aoki, Solid State Commun. **77**, 87 (1991).
[32] F.-J. Niedernostheide, J. Hirschinger, W. Prettl, V. Novák, and H. Kostial, Phys. Rev. B **58**, 4454 (1998).
[33] G. Hüpper and E. Schöll, Phys. Rev. Lett. **66**, 2372 (1991).
[34] E. Schöll, G. Hüpper, and A. Rein, Semicond. Sci. Technol. **7**, B480 (1992).
[35] R. M. Westervelt and S. W. Teltsworth, J. Appl. Phys. **57**, 5457 (1985).
[36] K. Aoki, *Nonlinear Dynamics and Chaos in Semiconductors* (IOP, Bristol, 2000).